

# Temporal thermal fluid analysis - An analytical approach

W E Sousa\*, S O Vellozo\*, R G Cabral\*

Nuclear Engineering Section, Military Institute of Engineering, Rio de Janeiro, Brazil,

\*walinton.evangelista@ime.eb.br, \*vellozo@cbpf.br, \*rgcabral@ime.eb.br

**ABSTRACT:** We analyzed two postulated transients of the European Sodium Fast Reactor (ESFR). Both heat conduction equations of the fuel pellet and the cooling, in this case sodium, and the punctual kinetics equations are used to estimate the power or temperature distribution in the fuel channel. We used two ESFR postulated accidents as benchmark. The highest percentage deviations were < 13%.

**KEYWORDS:** Regenerating Reactor, Temporal Thermal Fluid Analysis, Kinetics of Reactors.

**RESUMO:** Esse trabalho analisa dois transientes postulados do European Sodium Fast Reactor (ESFR). Tanto as equações de condução de calor da pastilha de combustível até o refrigerante, no caso, o sódio, assim como as equações da Cinética Pontual, são utilizadas para estimar a potência ou a distribuição de temperatura no canal do combustível. Dois acidentes postulados do ESFR foram utilizados como benchmark. Os maiores desvios percentuais verificados ficaram abaixo de 13%.

**PALAVRAS-CHAVE:** Reator Regenerador, Análise Termofluida Temporal, Cinética de reatores.

## 1. Introduction

The proper functioning of a nuclear reactor requires the removal of all the heat generated in the nucleus at the same rate at which it is generated. This characterizes the “stationary” state. The agent responsible for this heat removal is the cooling, which can be liquid or gaseous. However, the power level of the reactor can increase or decrease during operation to meet the daily energy demand, which characterizes “operational transients”. These transients momentarily happen in an intentional and programmed way when the reactor power level varies, thus causing an imbalance between the rates of heat production and removal in the core.

In other situations, this imbalance is not intentional or programmed and the reactor must quickly respond to restore the balance without damaging any components. We call this an “incident.”

In a more extreme situation, this imbalance between heat production and removal can cause irreversible damage to the nucleus, such as the rupture of the fuel rod’s coating, fusion etc., which is named an “accident”. The reactor’s Heat Removal System must ensure the protection of the reactor in any severe event.

## 1.1 Related Studies

Following the innovative line, the Military Institute of Engineering (IME) have been developing a conceptual design of a fast spectrum reactor without enriched uranium to implement it in the Brazilian nuclear park, which has required precise calculations to determine the void reactivity coefficient for the FBR-IME fast spectrum reactor and the thermal hydraulic analysis of Sodium.

In a first study, the conceptual design of a Liquid Sodium-Cooled Regenerating Fast Reactor, regardless of the enrichment technology, was elaborated. Its fuel is the mixture of oxides (MOX), which is the portion of plutonium and coming from the tailings of Thermal Reactors. All uranium used in the fuel and in the blanket has U-235 in its natural content. The SCALE 6 computer system of the Oak Ridge National Laboratory was used to develop the project. The designed reactor has a small heterogeneous nucleus and a common fuel management system at the end of its 360-day cycles [1].

In a second study, a global analysis of the void reactivity coefficient for the FBR-IME fast spectrum reactor was performed. For this, the FBR reactor was

modeled in the SCALE 6.1 system. Based on previous studies, the void insertion method, the reactivity of each configuration, the void reactivity coefficients in different configurations and the safety level of the FBR design toward the void reactivity coefficient [2] were determined.

In a third study, the preliminary thermal fluid analysis of sodium of the FBR-IME fast spectrum reactor was conducted [3].

## 2. Heat transfer

The temperature profiles were estimated, and its starting point was the central axis of the fuel pellet, in which the maximum temperature occurs up to the surface of the coating. From the coating onwards, the heat is removed by the convection process and a set of physical and geometric properties and flow of the fluid ensure this process.

The analysis of the hot channel of the fast reactor's nucleus, cooled by the sodium, does not differ from a common reactor. The heat generated by the fuel pellets reaches the surface of the coating (Clad).

Not all heat generated in the fuel pellets can be entirely removed by the cooling. There may be specific points in which the generated heat rate is higher than the rate of the heat removed by the cooling. These cases are analyzed in the next sections.

### 2.1 The energy balance in the fuel

This section shows the development of the temperature distribution in the stationary and transient states.

#### 2.1.1 The stationary

The balance equation establishes that the heat that escapes from a volume element must be equal to what is produced. As stated in Eq. 1:

$$FO = \sum_{i=1}^{NSites} PSI(Xd(i)=1,i), \quad (1)$$

The solution of Equation 1 is the temperature distribution within the fuel (Equation 2),  $f(r)$ :

$$\sum_{i=1}^{NSites} Xd(i) = NAAA, \quad (2)$$

In which  $T_{c_l}$  is defined as the temperature of the central line of the fuel;  $Q_0$  is the power density in that region;  $K_f$  is the heat conduction coefficient of the fuel; and  $r$  is the distance from the central line.

Therefore, the temperature distribution in the balance is a perfect parabola.

#### 2.1.2 The transient

The imbalance between heat production and its removal leads to temperature variation in the many regions of the fuel cell channel. The equation of heat conduction in the fuel is (Equation 3):

$$\rho_f c_p \left( \frac{\partial T_f(r,t)}{\partial t} \right) = K_f \nabla^2 T_f(r,t) + Q(t) \quad (3)$$

In which  $\rho_f$  is the mean density;  $c_p$  is the specific heat;  $K_f$  is the mean heat conduction coefficient in the fuel;  $Q(t)$  is the power density; and  $T_f(r,t) = f(r)T_f(t)$  is the temperature distribution in the fuel.

We found the final temporal general solution by separating the variables to solve the partial differential equation (Equation 3), which is (Equation 4):

$$T_f(t) = e^{at} \left\{ T(0) + b \int_0^t e^{-at'} Q(t') dt' \right\} \quad (4)$$

In which  $T(0) = 1$ ,  $a = \frac{Q_0}{\rho_f c_p \langle f \rangle}$ ;  $b = \frac{1}{\rho_f c_p \langle f \rangle}$ ;

$\langle f \rangle = T_{c_l} - \frac{Q_0}{8K_f} R_f^2$ ; and  $R_f$  is the radius of the fuel pellet.

The form of the heat generation rate  $Q(t)$  will define the profile of the temporal evolution of the temperature, and Equation 4 is the center of this evolution.

## 2.2 The Coating

### 2.2.1 The stationary

The heat conduction equation takes the following form in the absence of a source (Equation 5):

$$K_{rv} \nabla^2 T_{rv}(r) = 0 \quad (5)$$

By solving Equation 5 and performing some algebraic manipulations, the following expression for the temperature distribution in the coating is found, in which  $T_{rv}(r)$  can be written as shown in Equation 6:

$$T_{rv}(r) = T_0 - \frac{Q_0 R_{rv}^2}{2} \left\{ \frac{r - R_f}{R_f} \frac{1}{K_{rv}} + \frac{1}{2K_f} \right\} \quad (6)$$

In which  $T_0$  is the initial temperature,  $Q_0$  is the power density in that region;  $R_{rv}$  is the radius of the coating;  $R_f$  is the radius of the fuel pellet;  $K_{rv}$  is the mean heat conduction coefficient in the coating;  $K_f$  is the mean heat conduction coefficient in the fuel; and  $r$  is the radius.

### 2.2.2 The transient

This is the temporal evolution of the temperature distribution in the coating. Equation 7 shows the model:

$$\rho_{rv} c_{rv} \left( \frac{\partial T_{rv}(r,t)}{\partial t} \right) = K_{rv} \nabla^2 T_{rv}(r,t) \quad (7)$$

Based on the continuity of the temperature and heat flow in  $R_p$ , the solution of Equation 7 takes the following form after simplification (Equation 8):

$$T_c(r,t) = T_f(t) \left\{ f_f(R_f) + m(r - R_f) \right\} \quad (8)$$

Eq. 8 shows that the  $T_f(t)$  of the fuel determines the temporal evolution of the temperature distribution in the coating. Besides, the angular coefficient of this distribution,  $m = \frac{K_f}{K_c} \frac{df_f(R_f)}{dr}$ , depends on the ratio between the heat conduction coefficients of the fuel and the coating.

### 2.3 Heat Equations for Cooling

This section is about the temperature distribution in the cooling and the heat convection and conduction process from the coating to the cooling.

The following equation is to describe the temperature distribution in the cooling (Equation 9):

$$\left( \rho c_p \right)_f \left( \frac{\partial T_f}{\partial t} + \vec{v} \cdot \nabla T_f \right) = K_f \nabla^2 T_f \quad (9)$$

In this equation,  $\rho$  represents the mean density of the cooling fluid,  $c_p$  is the specific heat in constant pressure;  $\vec{v}$  is the mean speed of flow of this fluid;  $K_f$  is the heat conduction coefficient; and  $T_f$  is the temperature distribution within the cooling.  $T_f$  depends on the variables  $r$ ,  $z$  and  $t$ , that is,  $T_f = T_f(r, z, t)$ .

#### 2.3.1 The stationary regime

For the stationary regime, the energy balance equation is enough to determine the axial distribution of the cooling temperature. The integration into the volume element of the cooling  $dV = 2\pi r dr dz$  will leave the temperature dependent only on  $z$ . Thus, Equation 10 is written as follows:

$$dz \frac{dQ}{dt} = \dot{m} c_{fl} \frac{dT_{fl}}{dz} = q(z) dz \quad (10)$$

In which  $q(z) = q_0 \cos\left(\frac{\pi}{H} z\right)$ ;  $q_0 = Q_0 \pi (R_f)^2$ ;  $\dot{m} = v_z A \rho_{fl}$  is the mass flow rate;  $\rho_{fl}$  is the density of the cooling liquid sodium; and  $A$  is the cross-sectional area of the channel.

Integration into the active part of the channel leads to the following solution (Equation 11):

$$T_{fl} = T_m - \frac{Q_0 \tilde{H}}{\dot{m} c_{fl} \pi} \left\{ \text{sen}\left(\frac{\pi}{\tilde{H}} z\right) + \text{sen}\left(\frac{\pi H}{2 \tilde{H}}\right) \right\} \quad (11)$$

In which  $\tilde{H}$  is the extrapolated length of the rod and  $H$  is the actual length. All the heat generated in the fuel must reach the cooling in the stationary regime, and this heat can be accounted by the linear power density  $q(z) = q_0$ , in which  $q_0 = Q_0 \pi (R_f)^2$ .

#### 2.3.2 The Transient Cooling Regime

The study of the temporal evolution of the cooling is very simplified because liquid metal has a very high heat conduction coefficient compared to other materials, such as sodium, whose thermal conductivity is about  $76.6 \frac{W}{K \cdot m^2}$  to  $400^\circ C$ . In contrast, the conductivity of the water varies between  $0.6 \frac{W}{K \cdot m^2}$  to  $20^\circ C$  and  $0.465 \frac{W}{K \cdot m^2}$  to  $350^\circ C$  (under a pressure of 150 bar). The conductivity of sodium is 100 to 150 times higher than atmospheric pressure [4]. Therefore,

the temperature quickly equalizes in the volume element cross-sectional to the axis. The consideration of a mean temperature in each axial elementary volume is valid [6][7].

A convection coefficient will represent the heat transfer from the coating to the cooling  $h_s \left[ \frac{W}{Km^2} \right]$ . The heat flow per unit area is determined by the product between the heat transfer coefficient and the difference between the temperature of the wall of the coating and the mean cooling temperature (Newton's cooling law), as shown in Equation 12.

$$q'' = h_s (T_{rv}(R_{rv}) - T_{fl}) \quad (12)$$

The convection coefficient is estimated by  $h_s = k_s \frac{Nu}{D_h}$ , in which  $k_s$  is the sodium's heat conduction coefficient;  $D_h$  is the hydraulic diameter; and  $Nu$  is the Nusselt number for each fuel assembly arrangement, with correlation by Todreas and Kazimi,  $Nu = 7 + (0.025)(Pr)(Re)$ , in which  $Pr$  and  $Re$  are the Prandtl and Reynolds numbers, respectively.

### 3. The ESFR reactor

The ESFR [8] is a fast spectrum regenerating reactor in development in Europe. It uses uranium and plutonium oxides-based fuel. The reactor power is 3,600 MWth and the active length of the core is only 1 m. The main characteristics of our study, for neutron modeling purposes, can be found in the reference [9]. **Tables 1** and **2** show the data used in the simulations. They show the analysis of two major accidents using the AZTH-LIM code. It models the heat transfer processes in the cooling (liquid metal) of the ESFR fast reactor, considering heat transfer in the fuel bar and the neutron processes. The first accident is the ejection of an absorbing bar with the introduction of 175 pcm of reactivity, which is an Unprotected Transient Over-Power (UTOP). The second accident is a 50% loss of the pump power and is called a thermal fluid Unprotected Loss-Of-Flow (ULOF). The results, benchmark, of these postulated and estimated accidents [8] will be the basis for comparison in our study's analytical simulations.

A **Table 1** shows the main parameters of the European reactor used in the simulations.

**Tab. 1** - Main ESFR parameters

Power	3,600 MWth	Radius of the central hole	0.1257 cm
Active height	1.00566 m	Fuel radius	0.4742 cm
Entrance temp.	668.15 K	Coating radius	0.5419 cm
Exit temp.	818.15 K	Step	1.1897 cm
Mean temp. of the fuel	818.15 K	Cells per EC	271 un
Mass flow rate	19,000 kg/s	EC number	453 un

**Table 2** shows the fuel properties.

**Tab. 2** - ESFR Fuel Properties

Properties	Correlation
Density (kg/m <sup>3</sup> )	$\rho_f = \frac{11043,5}{(0,99672 + 1,179 \times 10^{-5}T - 2,428 \times 10^{-9}T^2 - 1,219 \times 10^{-9}T^3)^3}$
Specific heat (J/kg K)	$C_f = 0,85 \times \left( \frac{0,998 \times 10^6 A}{(A-1)T^2} + 1,6926 \times 10^{-2}T + \frac{1,620 \times 10^{12}}{T^2} \right) + 0,15 \times \left( \frac{111,275 \times 10^{12} B}{(B-1)T^2} + 2,9358 \times 10^{-2}T \right)$
Heat Transfer Coef. (W/m K)	$K_f = 1,158 \times \left( \frac{1}{0,1205 + 2,6455 \times 10^{-2}T} + \frac{6400e^{-\frac{16,33}{T}}}{\tau^{\frac{5}{2}}} \right)$ $A = e^{\frac{548,68}{T}} ; B = e^{-\frac{18541,7}{T}} ; \tau = \frac{T}{1000}$

### 4. Analytical simulations

In analytical simulations, Equation 4 is essential to describe temporal evolution. Both transients will be studied and compared to the ESFR results taken as a reference, benchmark.

#### 4.1 Insertion of 175 pcm due to bar ejection

T function (t), Equation 4, which describes temporal evolution, must be estimated according to Q(t). The latter is obtained by adjusting to the EFSR power curve. The adjusted function has the following form:

$$\frac{Q(t)}{Q_0} = 1,26 + 0,49e^{-0,3t^2} \quad (13)$$

**Figure 1** shows the comparison between adjustment and benchmark:

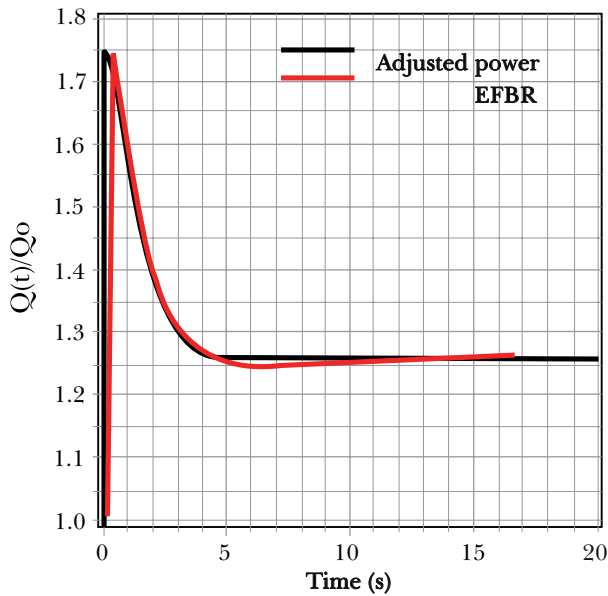


**Fig. 1** - Normalized power profile adjusted for a reactivity insertion of 175 pcm.

**Figure 2** shows the mean fuel temperature estimated in the ESFR (red curve). The transient starts at approximately five seconds and the temperature reaches a maximum of approximately 1,700 K and stabilizes just below that value.

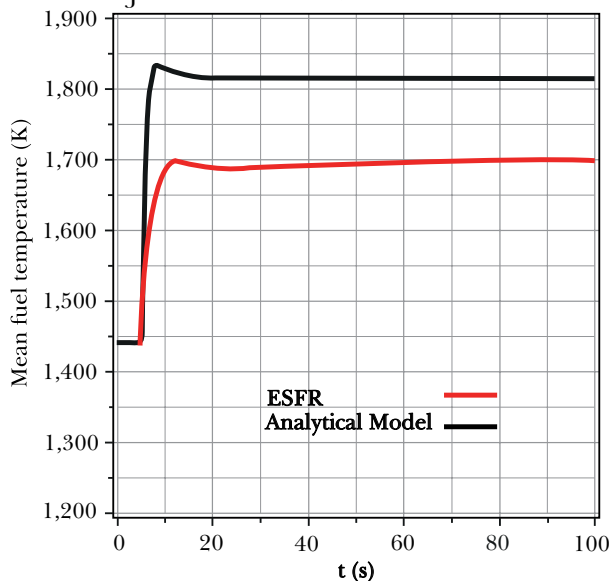


**Fig. 2** - Mean fuel temperature.

**Figure 2** shows that the analytical model is conservative, exceeding the maximum value of

the mean fuel temperature by just over 100 K and stabilized just above 1,800 K (black curve). This represents approximately a 6% difference compared to the ESFR result with benchmark, if the entire temperature range is considered.

The analytical model qualitatively represented, with reasonable fidelity, the inertia of the mean temperature characterized by the initial peak of the curve.

**Figure 2** shows the mean fuel temperatures, simulated with the proposed analytical model and with the ESFR data.

#### 4.2 Loss of 50% of flow rate

The second studied transient refers to the loss of flow rate in the fuel channel. **Figure 3** shows the curves of the axial temperature distribution in the sodium in the normal flow rate and with 50% ESFR loss estimated by the AZTHLIM code. The temperature at the tip of the channel reaches 881.35 K.

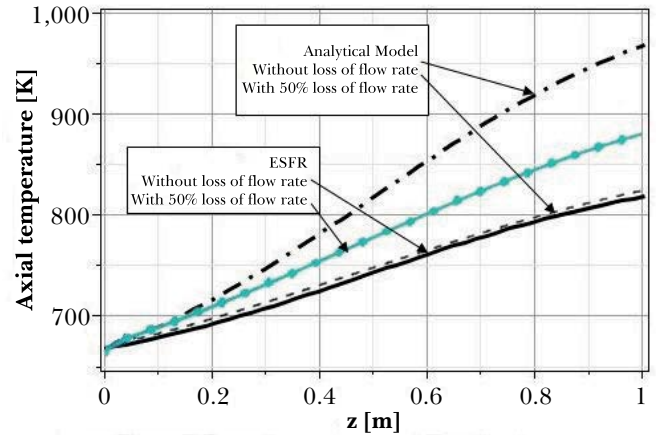


**Fig. 3** - Axial temperature of sodium for a 50% loss of flow rate estimated by the analytical model and the AZTHLIM code.

The analytical model maintains the conservative tendency. **Figure 3** shows the behavior of temperature distribution in cases of normal flow rate and with 50% loss of flow rate. The temperature at the tip of the channel reached just over 950 K, which is a difference of approximately 13% compared to ESFR.

**Figure 3** shows the axial temperature of sodium for a 50% loss of flow rate.

## 5. Conclusion

The analytical model is limited, although the analyzed results showed deviations lower than 13% compared to the European ESFR reactor, used as a

benchmark. Therefore, quick analyses are possible when the main goal is to know the superior limiters for a transient. An analysis conducted by a detailed and numerically resolved model will establish reliable values, reducing costs to the project.

## References

- [1] OLIVEIRA, Aline Alves. **Reator rápido regenerador independente de urânio enriquecido**. Rio de Janeiro: Instituto Militar de Engenharia, 2014.
- [2] LIMA, Fabiano Petruceli Coelho. **Análise global do coeficiente de reatividade de vazios para o reator de espectro rápido FBR-IME**. Rio de Janeiro: Instituto Militar de Engenharia, 2018.
- [3] VELOSO, Marta Jan. **Análise termofluida preliminar do reator de espectro rápido FBR-IME**. Rio de Janeiro: Instituto Militar de Engenharia, 2018
- [4] BALDEV Raj, et al. **Sodium Fast Reactors with Closed Fuel Cycles**, CRC Press. Florida: Taylor and Francis-Group, 2015.
- [5] BERTHOUD, et al.,. **Sodium-cooled nuclear reactors**. France: Editions Le Moniteur, 2014.
- [6] WALTAR, A.E. et al. **Fast Spectrum Reactors**. 1ªEd. Richland: Springer, 2012.
- [7] TODREAS, N., Kazimi, M. **Nuclear Systems: Thermal Hydraulic Fundamentals**. Nuclear Systems. Hemisphere Pub. Corp. 1990.
- [8] FACCHINI, A., GIUSTI, V., CIOLINI R., TUCEK, K., THOMAS, D., D'AGATA, E. Detailed neutronic study of the power evolution for the European Sodium Fast Reactor during a positive insertion of reactivity. **Nuclear Engineering and Design**, 313, 2017, pp.1–9.
- [9] VALSECA, A. D. P., PAREDES, G. E., RODRÍGUEZ, A. V. Analysis of a Sodium Cooled Fast Reactor during ULOP and UTOP Transients Using AZTHLIM Code. **XXIX Congreso Anual de la Sociedad Nuclear Mexicana**, 2018.